Journal of Coordination Chemistry

Synthesis, structures and luminescence properties of two gallium(III) complexes with 5,7-dimethyl-8-hydroxyquinoline

Orbett T. Alexander, Mart M. Duvenhage, Alice Brink, Hendrik C. Swart, Peter Müller, R. E. Kroon & Hendrik G. Visser

View supplementary material

Submit your article to this journal

View related articles

Citing articles: 4 View citing articles

Accepted author version posted online: 07 Mar 2017.
Published online: 22 Mar 2017.

Article views: 184

View Crossmark data

Taylor & Francis
Taylor & Francis Group

Check for updates

Synthesis, structures and luminescence properties of two gallium(III) complexes with 5,7-dimethyl-8-hydroxyquinoline

Orbett T. Alexander[a], Mart M. Duvenhage[b], Alice Brink[a], Hendrik C. Swart[b] iD, Peter Müller[c], R. E. Kroon[b] and Hendrik G. Visser[a]

[a]Department of Chemistry, University of the Free State, Bloemfontein, South Africa; [b]Department of Physics, University of the Free State, Bloemfontein, South Africa; [c]Department of Chemistry, Massachusetts Institute of Technology, Cambridge, MA, USA

ABSTRACT

Luminescent gallium(III) complexes featuring 5,7-dimethyl-8-hydroxyquinoline (DimOx) are systematically compared and their structural features are correlated with their photophysical properties. The two complexes are chemically identical; however, contain various number of solvent molecules in the crystalline lattice which is representative of the bulk material confirmed by both nuclear magnetic resonance and elemental analysis. Detailed structural comparisons highlight the effect which the solvent molecules have on the intra- and intermolecular interactions. A distinct number of interactions are found for the gallium complex (**1**) containing more than one solvent molecule for unit cell. Variation in complex morphology is similarly observed via SEM micrographs. The distinct luminescent properties of the two gallium complexes appear directly related to octahedral coordination of the 8-hydroxyquinoline ligand as well as the number of identical coordinated solvent molecules.
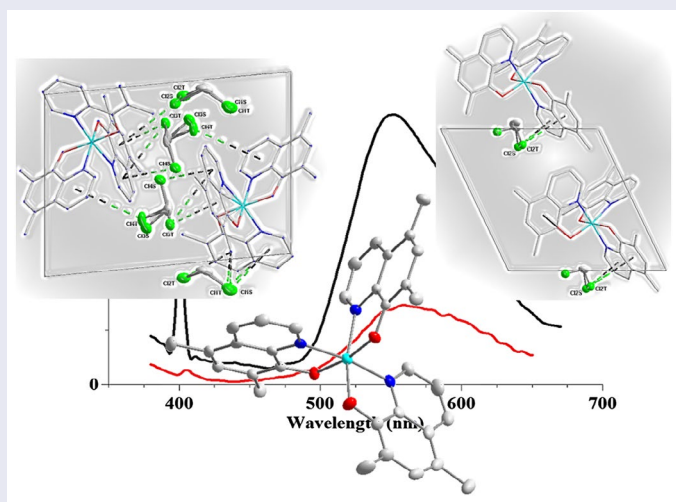
1. Introduction

The luminescent properties of metal complexes coordinated to 8-hydroxyquinoline (Ox) and derivatives thereof play an important role in optical electronics applications such as organic light-emitting diodes (OLEDs), since Tang and Van Slyke first reported the chemical luminescence of [Al(Ox)$_3$] [1–8].

The effectiveness of [M(Ox)$_3$] (M = aluminum, gallium, indium) complexes as OLED's depends on several factors, including whether facial (*fac*) or meridional (*mer*) coordination isomers are isolated, whether there are solvents trapped in the crystal lattice, the type of inter- and intramolecular interactions, *etc.* [9–11]. In general, *fac*-isomers are preferred due to their blue-shifted fluorescence and reasonably high quantum yields. For aluminum, especially, these complexes are normally synthesized as *mer*-isomers which can be converted to *fac*-complexes by high temperature sublimation [12, 13].

In the case of 8-hyxdroxyquinoline it has been shown that the luminescent properties of metal complexes can be red- or blue-shifted by varying the electronic properties of the substituents on the ligand backbone [14, 15]. OLEDs containing gallium tend to exhibit higher electroluminescent yields than equivalent metal centers, such as aluminum or indium [16, 17]. The correlations between the molecular packing of [Al(Ox)$_3$]·solvent complexes and optical properties have been investigated [10]. It was found that fluorescence of non-solvated compounds is substantially red-shifted and that of solvated structures tend towards blue-shifted fluorescence. The red shift was attributed to shorter π–π interactions resulting in higher crystal density. Trapped guest molecules on the other hand tend to behave like spacer molecules and eventually elongate the π–π contact distances. That could sway the shift in the reverse manner in some cases but also increase the photoluminescence intensity in others, depending on the type of interactions between the molecules [18–20].

Our interest lies in basic understanding of the synthesis and structural properties which influence the luminescence of these types of complexes. The synthesis, X-ray crystallographic structures and luminescence properties of two gallium(III) complexes containing the 5,7-dimethyl-8-hydroxyquinoline (DimOx), *mer*-[Ga(DimOx)$_3$]·CH$_2$Cl$_2$ and *mer*-[Ga(DimOx)$_3$]·2CH$_2$Cl$_2$ are reported here. The serendipitous discovery of single crystals with a different number of dichloromethane solvent molecules in the crystal lattice provides the rare opportunity to investigate solvent effects in photoluminescence unequivocally.

2. Experimental

2.1. General procedures and materials

Unless otherwise stated, all reagents used for synthesis and characterization were of reagent grade, purchased from Sigma-Aldrich. Reagents were used as received, without purification unless deemed necessary. ^{13}C and ^{1}H FT-NMR spectra were recorded at 150.96 and 600.28 MHz, respectively, on a Bruker 600 MHz or 300 MHz at 25 °C in CDCl$_3$ (7.26 ppm); chemical shifts are reported in ppm. All data were recorded at room temperature. UV-vis spectra were collected on a Varian Cary 50 conc. UV-visible spectrophotometer equipped with a Julabo F12-mV temperature cell regulator (accurate within 0.05 °C) in a 1.000 ± 0.001 cm quartz cuvette cell.

2.2. Synthesis of mer-[Ga(DimOx)$_3$]·2CH$_2$Cl$_2$ (1)

Ga(NO$_3$)$_3$·H$_2$O (0.35 g, 1.37 mmol) dissolved in 20 mL of distilled water was added to a solution of 5,7-dimethyl-8-hydroxyquinoline (0.711 g, 4.11 mmol) dissolved in 15 mL of water. The pH of the solution was adjusted to 8 by dropwise addition of NaOH (2 M). The formed precipitate was filtered and dried in vacuo. Crystals of **1** were obtained after two days by recrystallization from dichloromethane at room temperature (81%). *Anal. Calc.* for GaCl$_4$N$_3$O$_3$C$_{35}$H$_{34}$: C, 55.6; H, 4.5; N, 5.6. Found: C, 55.5; H, 2.6; N, 5.7. UV-vis (nm; L mol^{-1} cm^{-1}): λ_{max} = 408.1, ε = 8.8 × 10^3, λ_{max} = 340, ε = 4.9 × 10^3, λ_{max} = 324, ε = 4.7 × 10^3. ^{1}H NMR (600 MHz, CDCl$_3$) δ: 8.85 (d, J = 3.8 Hz, 1H), 8.74 (d, J = 3.9 Hz, 1H), 8.35 (d, J = 8.5 Hz, 1H), 8.33 (d, J = 8.2 Hz, 1H), 8.29 (d, J = 9.0 Hz, 1H), 7.38 (dd, J = 8.5, 4.7 Hz, 1H), 7.36 – 7.33 (m, 1H), 7.33 – 7.30 (m, 1H), 7.17 (dd, J = 8.1, 4.4 Hz, 1H), 5.23 (s, 4H), 2.52 (s, 3H), 2.49 (d, J = 2.7 Hz, 6H), 2.40 (s, 3H), 2.39 (d, J = 2.4 Hz, 6H). ^{13}C NMR (151 MHz, CDCl$_3$) δ: 156.8, 154.8, 154.1, 151.5, 147.7, 145.3, 144.0, 143.9, 142.9, 141.7, 141.6, 137.0, 136.6, 136.5, 136.4, 133.6, 133.6, 133.4, 133.1, 127.2, 127.1, 126.8, 121.8, 121.6, 121.1, 120.06, 119.9, 119.3, 117.4, 53.5, 17.7, 17.6, 17.5, 17.0, 16.9, 16.8.

2.3. Synthesis of mer-[Ga(DimOx)$_3$]·CH$_2$Cl$_2$ (2)

Ga(NO$_3$)$_3$·H$_2$O (0.35 g, 1.37 mmol) dissolved in 20 mL of distilled water was added to a solution of 5,7-dimethyl-8-hydroxyquinoline (0.711 g, 4.11 mmol) dissolved in 15 mL of a 2 M NaOH solution in water. The formed precipitate was filtered and dried in vacuo. Crystals of **2** were obtained after one week by recrystallization from a mixture of dichloromethane and methanol at 0 °C (65%). *Anal. Calc.* for GaN$_3$O$_3$C$_{34}$H$_{32}$Cl$_2$: C, 60.8; H, 4.8; N, 6.3. Found: C, 61.0; H, 4.6; N, 6.2. UV-vis (nm; L mol^{-1} cm^{-1}): λ_{max} = 408.1, ε = 8.8 × 10^3, λ_{max} = 340, ε = 4.9 × 10^3, λ_{max} = 324, ε = 4.7 × 10^3. ^{1}H NMR (600 MHz, CDCl$_3$) δ: 8.85 (d, J = 3.8 Hz, 1H), 8.74 (d, J = 3.9 Hz, 1H), 8.35 (d, J = 8.5 Hz, 1H), 8.33 (d, J = 8.2 Hz, 1H), 8.29 (d, J = 9.0 Hz, 1H), 7.38 (dd, J = 8.5, 4.7 Hz, 1H), 7.36 – 7.33 (m, 1H), 7.33 – 7.30 (m, 1H), 7.17 (dd, J = 8.1, 4.4 Hz, 1H), 5.23 (s, 2H), 2.52 (s, 3H), 2.49 (d, J = 2.7 Hz, 6H), 2.40 (s, 3H), 2.39 (d, J = 2.4 Hz, 6H). ^{13}C NMR (151 MHz, CDCl$_3$) δ: 156.8, 154.8, 154.1, 151.5, 147.7, 145.3, 144.0, 143.9, 142.9, 141.7, 141.6, 137.0, 136.6, 136.5, 136.4, 133.6, 133.6, 133.4, 133.1, 127.2, 127.1, 126.8, 121.8, 121.6, 121.1, 120.06, 119.9, 119.3, 117.4, 53.5, 17.7, 17.6, 17.5, 17.0, 16.9, 16.8.

2.4. Analytical techniques

2.4.1. X-ray crystallography

Diffraction data for **1** and **2** were collected on a Bruker ApexII 4 K CCD diffractometer using Mo-Kα (0.71073 Å) φ and ω-scans at 100 K. Data reduction was performed with SAINT-PLUS [21] and absorption correction and scaling were performed with SADABS [22]. Both structures were solved by the heavy atom method using SHELXS. Structures were refined with SHELXL-2014 [23] through full-matrix least-squares against F^2 using all data and applying established refinement techniques [24]. All non-hydrogen atoms were refined with anisotropic displacement parameters. All hydrogens were placed in geometrically calculated positions and refined using a riding model while constraining their U_{iso} to 1.2 times the U_{eq} of the atoms to which they bind (1.5 times for methyl groups). The graphics were obtained with the visual crystal structure information system software DIAMOND [25]; crystallographic details are summarized in table 1. Selected bond lengths and angles of **1** and **2** are listed in tables 2 and 3, respectively.

Table 1. Crystal data and structure refinements for **1** and **2**.

Compound	1	2
Empirical formula	$GaCl_4N_3O_3C_{35}H_{34}$	$GaN_3O_3C_{34}H_{32}Cl_2$
Formula weight	756.17	671.25
Temperature (K)	100(2)	100(2)
Wavelength (Å)	0.71073	0.71073
Crystal system	Triclinic	Triclinic
Space group	$P\bar{1}$	$P\bar{1}$
Unit cell dimensions (Å, °)		
a	11.368(2)	11.217(5)
b	11.374(2)	11.283(5)
c	14.659(3)	13.660(5)
α	88.32(3)	101.315(5)
β	74.40(3)	97.324(5)
γ	65.64(3)	113.366(5)
Z	2	2
Volume ($Å^3$)	1655.8(6)	1515.2(11)
Calculated density (g cm^{-1})	1.517	1.47
Absorption coefficient ($Lmol^{-1}$ cm^{-1})	1.195	1.125
$F(0\,0\,0)$	776	692
Crystal color	Yellow	Yellow
Crystal morphology	Needle	Block
Crystal size (mm^3)	$0.195 \times 0.125 \times 0.105$	$0.200 \times 0.200 \times 0.200$
θ range for data collection (°)	1.97–28.30	2.03–28.31
Completeness (%)	99.6	99.4
Index ranges		
h	−14 to 15	−14 to 14
k	−15 to 15	−15 to 15
l	−19 to 19	−18 to 18
Reflections collected	30,488	21,138
Independent reflections	8172 [R(int) = 0.0238]	7404 [R(int) = 0.0422]
Refinement method	Full-matrix least-squares on F^2	Full-matrix least-squares on F^2
Data/restraints/parameters	8172/993/618	5476/811/528
Goodness-of-fit on F^2	1.088	1.076
Final R indices [I > 2σ(I)]	$R_1 = 0.0326, wR_2 = 0.0766$	$R_1 = 0.0495, wR_2 = 0.1086$
R indices (all data)	$R_1 = 0.0386, wR_2 = 0.0790$	$R_1 = 0.0826, wR_2 = 0.1222$
Largest diff. peak and hole (e $Å^3$)	0.409 and −0.310	0.869 and −0.772

Table 2. Selected bond lengths and angles for **1**.

Bond	d (Å)	Bond	d (Å)
Ga1–O1	1.9526(13)	Ga1–N1	2.0658(15)
Ga1–O2	1.9428(15)	Ga1–N2	2.0913(15)
Ga1–O3	1.9442(17)	Ga1–N3	2.102(3)
Angle	ω (°)	Angle	ω (°)
O1–Ga1–N1	82.35(6)	O2–Ga1–O1	96.40(6)
O1–Ga1–N2	94.63(6)	O3–Ga1–O2	90.05(8)
O1–Ga1–N3	92.77(8)	O1–Ga1–O3	170.62(6)
N1–Ga1–N2	173.98(6)	O2–Ga1–N2	81.71(6)
N1–Ga1–N3	94.79(9)	O3–Ga1–N3	81.80(9)

2.4.2. Luminescence studies

Fluorescence spectra were collected on a Cary Eclipse fluorescence spectrophotometer with a 15 W Xenon flash lamp that flashes at a rate of 80 flashes per second with an average pulse width of 2–3 μs, as well as using an Edinburgh Instruments FLS980 fluorescence spectrophotometer having a 450 W steady state Xenon lamp. The latter was equipped with double excitation and double emission monochromators to minimize artifacts associated with

Table 3. Selected bond lengths and angles for **2**.

Bond	d (Å)	Bond	d (Å)
Ga1–O1	1.953(2)	Ga1–N1	2.092(3)
Ga1–O2	1.951(2)	Ga1–N2	2.072(3)
Ga1–O3	1.940(2)	Ga1–N3	2.105(4)
Angle	ω (°)	Angle	ω (°)
O1–Ga1–N1	81.57(10	O2–Ga1–O1	98.24(10)
O1–Ga1–N2	93.97(10)	O3–Ga1–O1	89.01(11)
O1–Ga1–N3	167.64(12)	O3–Ga1–O2	170.09(10)
N1–Ga1–N2	171.76(10)	O2–Ga1–N2	81.94(9)
N1–Ga1–N3	91.17(12)	O3–Ga1–N3	81.71(12)

strong scattering from powder samples and was also fitted with a 120 mm integrating sphere for the measurement of quantum yields.

2.4.3. SEM

The morphology of the samples was determined by scanning electron microscopy (SEM) using a JSM-7800F Extreme-resolution Analytical Field Emission SEM.

3. Results and discussion

3.1. Synthesis of gallium complexes

The synthesis and subsequent recrystallization of two *tris*-coordinated complexes of gallium(III) with 5,7-dimethyl-8-hydroxyquinoline yielded surprising results in that the only difference between **1** and **2** is the number of solvent molecules trapped in the crystal lattice. The results are supported by UV–vis, ^{1}H and ^{13}C NMR spectra and elemental analysis. Both **1** and **2** yield similar ^{1}H NMR spectra as expected and these spectra are indicative of the meridonial arrangements for the complexes in solution. Also evident from the spectra is the fact that the dichloromethane proton signal integrations correspond to the number of solvent molecules in **1** and **2**, indicating that the solvent dichloromethane molecules are not crystallographic anomalies but are representative of the bulk of both samples. The UV-vis spectra of **1** and **2** in methanol are similar with an intense band located at 408 nm reported to be a ligand-centered electronic transition [26] and two weak bands observed at 324 nm and 340 nm, respectively.

3.2. Crystallographic studies

The asymmetric unit of **1** contains one gallium(III) coordinated to three DimOx bidentate ligands to form a distorted octahedral arrangement as well as two CH_2Cl_2 solvent molecules (see figure 1 for atomic labeling scheme). One of the bidentate ligands is disordered (flipped over) over two positions. The disorder was refined with the help of similarity restraints for bond lengths and angles as well as similar ADP and rigid-bond restraints. The disorder ratio was refined freely and converged at 0.853(3), corresponding to a 85 : 15 disorder. This disorder superimposes the two alternative positions of the DimOx ligand in such a way that the meridonial stereochemistry of the main molecule remains intact (see figure 2). All discussion of molecular geometry is based solely on the major disorder component. The distortion around the metal center is illustrated by the Ga-O bond distances and angles (see
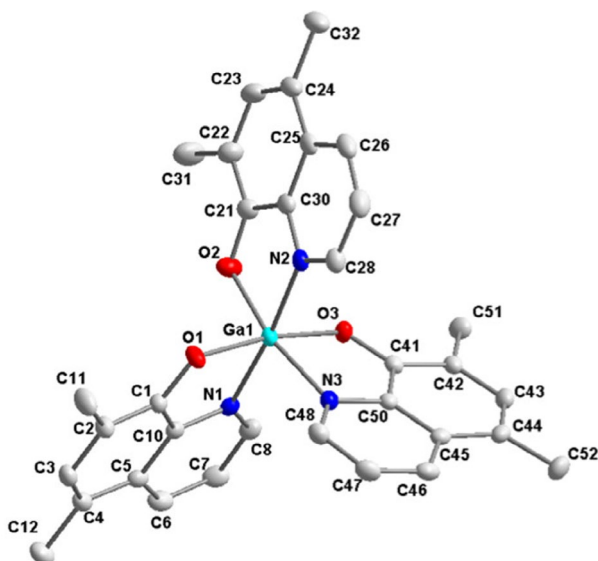
Figure 1. Atomic labeling scheme for the main part of **1**. Hydrogens and solvent molecules are omitted for clarity. Thermal ellipsoids are drawn at 50% probability.
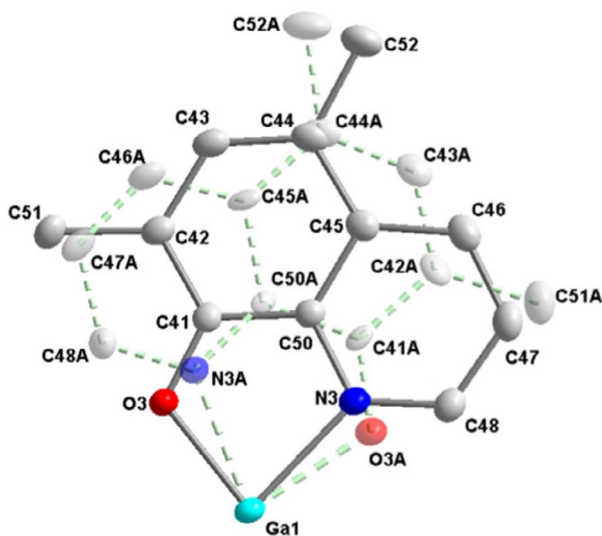

Figure 2. Illustration of the disorder in **1**. Hydrogens and solvent molecules are omitted for clarity. Thermal ellipsoids are drawn at 50% probability.

table 2) that vary from 1.9428(15) to 1.9526(13) Å (Ga1-O2 and Ga1-O1, respectively) and the O-Ga-O angles, 90.05(8) and 94.40(6)° (O2-Ga1-O3 and O2-Ga1-O1, respectively). All bond distances and angles correlate well with similar structures in the literature [27, 28]. Both solvent molecules are disordered, one over two, the other over three positions. The crystal structure is stabilized by C–H···Cl and C–H···O hydrogen bonds (table S1 in
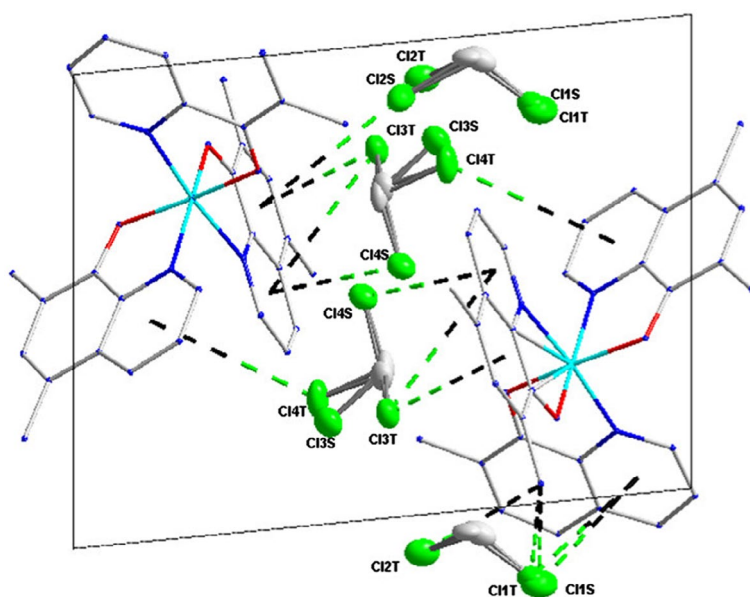
Figure 3. Cl···π interactions of **1** as viewed along the crystallographic *a*-axis.

Supplementary data) and a complex array of Cl···π interactions (table S2 in Supplementary data). The Cl···π interactions are illustrated in figure 3 as viewed along the crystallographic *a*-axis and illustrate the intermolecular interactions between the solvent species and the gallium molecule. The solvent molecules pack in columns between the complex molecules and as such, serve to stabilize the crystal structure.

The crystal structures of **1** and **2** are similar. The most prominent difference is the circumstance that there is only one CH_2Cl_2 solvent molecule in **2** (disordered over two positions) as opposed to two in **1**. The atomic labeling scheme for the structure of **2** is similar to the one used for the structure of **1** (see figure S1 in Supplementary data). The main molecule is disordered in the same way as described for the structure of molecule **1** and the disorder was refined the same way. The disorder ratio refined to 0.897(3), corresponding to a 90:10 disorder. All discussion of molecular geometry is based solely on the major disorder component. The distortion from octahedral geometry around gallium(III) are again illustrated by the deviations of the bond angles from 180° (see table 3). All bonding distances and angles in **2** compare well with those in **1** and similar structures. The crystal structure of **2** is stabilized by C–H···O hydrogen bonds and Cl···π interactions (see figure 4). Tables listing the geometrical parameters of these interactions are listed in the Supplementary data, tables S4 and S5. The Cl···π interactions are illustrated in figure 4 as viewed along the crystallographic *c*-axis. It is obvious from this figure that the intermolecular interactions between the solvent and the main molecule are less pronounced in the structure of **2** than in **1** since only two reasonable interactions are observed here.
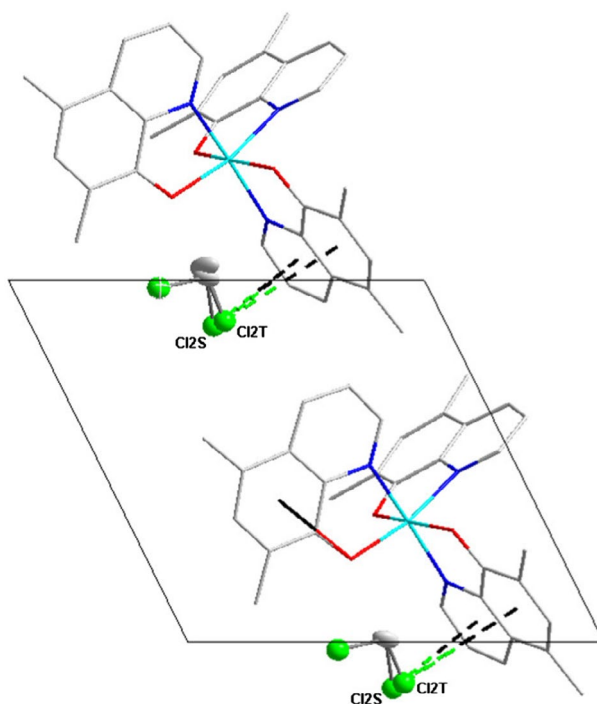
Figure 4. Cl···π interactions in the structure of **2** as viewed along the crystallographic *c*-axis.
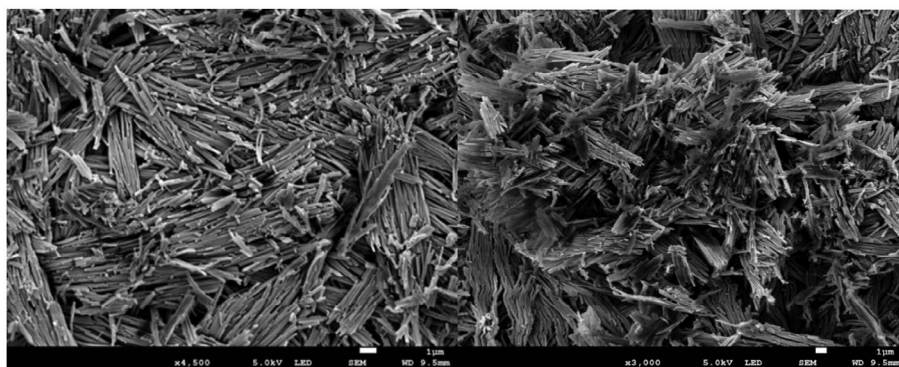

Figure 5a SEM micrographs for gallium complex **1**.

3.3. SEM spectroscopy

Illustrations of the SEM micrographs of **1** and **2** are indicated in figure 5(a) and 5(b). **1** shows sharp needle-like structures that are agglomerated to form plates. The needles are less than 1 μm thick. For **2**, big micron-sized particles are observed [29].

Several factors may affect the crystal growth or even crystal morphology of a material. These include solute–solvent interactions at various crystal–solution interfaces, which leads to altered interfaces, changes in crystal growth kinetics and enhancement [30] or inhibition [31] of growth at certain crystal faces. The fact that the morphology of **1** reveals plate-like
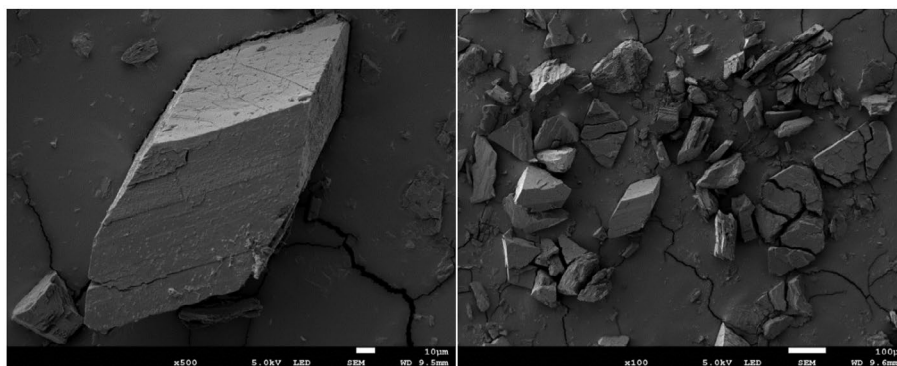
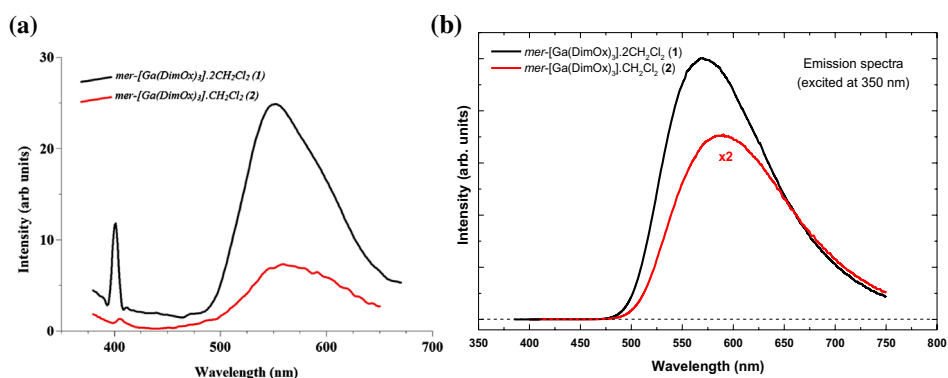**Figure 5b** SEM micrographs for gallium complex **2**.

Figure 6. Solid-state PL spectra of **1** and **2** (a) using the Cary Eclipse excited at 345 and 350 nm, respectively, and (b) using the Edinburgh Instruments FLS980 excited at 350 nm.

crystals could be due to faster crystallization (room temperature). In addition, **2** was re-crystallized from a mixture of methanol and dichloromethane as opposed to only dichloromethane in **1**.

3.4. Luminescence

The solid-state emission spectra of **1** and **2** are illustrated in figure 6. The data for figure 6(a) was collected using the Cary Eclipse fluorescence spectrophotometer and the samples were excited at respective wavelengths of 345 and 350 nm. This correlates with a higher energy electronic transition (S4 and above) [32, 33]. Both samples show emission at ~560 nm. The emission is due to the relaxation of an excited electron from the S1-S0 level. It is clear from figure 6(a) that the fluorescence intensity of **1** is much higher than **2**. This difference is attributed to the fact that **1** has more solvent molecules trapped in the crystal lattice. Although the small peak at ~400 nm has been attributed to the emission of 8-hydroxyquinoline [34], careful analysis shows that it varied significantly as the excitation was changed over the range 340–360 nm and is an instrument artifact due to the strong scattering of the powder samples. When measured for an excitation wavelength of 350 nm using the Edinburgh

Instruments FLS980 instrument, having double monochromators to better suppress stray light effects, the peak did not occur as shown in figure 6(b). Measurements with this system also showed that the emission from **1** is more than double of that of **2**, and that the peak intensities of the samples occurred at 570 nm and 590 nm after correction for the spectral response of the system. The quantum yield was assessed using a 120 mm integrating sphere by taking the ratio of the number of emitted photons to the absorbed photons (determined by comparing scans of the light source over the excitation range incident on the samples and a Spectralon™ standard), hence revealing that **1** has a quantum yield of 3.9% and **2** has a quantum yield of 1.8%.

Finally, the crystal density of **1** is calculated as 1.517 g cm^{-3} as opposed to 1.47 g.cm^{-3} for **2** (table 1). From this and from the crystallographic evaluation which showed substantially more solvent-to-parent-structure interactions in **1**, it can be deduced that the higher fluorescence efficiency of **1** is a direct result of denser packing and stabilization of the crystal structure due to the additional solvent molecule.

4. Conclusion

The distinct luminescent properties and crystal structures of two similar crystalline materials, differing only in the number of solvent molecules in the crystal lattice, were reported. It has been reported [10] that crystal density can influence the luminescence properties of materials. In terms of our results it is clear that **1** exhibits higher intensity as compared to **2** (figure 6) and has more intermolecular interactions, which would necessarily become stronger as molecules pack closer. The morphology of the used samples may also contribute to some extent to the differences in luminescence, with **1** being much finer than **2**, therefore providing a larger surface area which should increase the photoluminescence intensity.

Supplementary material

Supporting information for this article is given via a link at the end of the document. Crystallographic data for the structures **1** and **2** are available free of charge from the Cambridge Crystallographic Data Center via www.ccdc.cam.ac.uk/data_request/cif as CCDC 1460847−1460848.

ORCID

Hendrik C. Swart 🔟 http://orcid.org/0000-0001-5233-0130

References

[1] C.W. Tang, S.A. Van Slyke. *Appl. Phys.*, **51**, 913 (1987).
[2] Y. Wang, W. Zhang, Y. Li, L. Ye, G. Yang. *Chemistry of Materials*, **11**, 530 (1999).
[3] L.S. Sapochak, F.E. Benincasa, R.S. Schofield, J.L. Baker, K.K.C. Riccio, D. Fogarty, H. Kohlmann, K.F. Ferris, P.E. Burrows. *J. Am. Chem. Soc.*, **124**, 6119 (2002).
[4] P.J. Han, A.L. Rheingold, W.C. Trogler. *Inorg. Chem.*, **52**, 12033 (2013).
[5] F.J. Zhang, F.Y. Sun, Y.Z. Shi. *Energy Fuel*, **24**, 3739 (2010).
[6] L.S. Hung, C.W. Tang, M.G. Mason. *Appl. Phys. Lett.*, **70**, 152 (1997).
[7] H.Y. Chen, J.H. Hou, S.Q. Zhang. *Nat. Photonics*, **3**, 649 (2009).
[8] C. Dimitrakopoulos, P. Malenfant. *Adv. Mater.*, **14**, 99 (2002).
[9] T. Lee, M.S. Lin. *Cryst. Growth Des.*, **7**, 1803 (2007).
[10] M. Brinkmann, G. Gadret, M. Muccini, C. Taliani, N. Masciocchi, A. Sironi. *J. Am. Chem. Soc.*, **122**, 5147 (2000).
[11] M. Muccini, M.A. Loi, K. Kenevey, R. Zamboni, N. Masciocchi, A. Sironi. *Adv. Mater.*, **16**, 861 (2004).
[12] R. Katakura, Y. Koide. *Inorg. Chem.*, **45**, 5730 (2006).
[13] M. Cölle, J. Gmeiner, W. Milius, H. Hillebrecht, W. Brütting. *Adv. Func. Matter*, **13**, 108 (2003).
[14] F. Artizzu, M.L. Mercuri, A. Serpe, P. Deplano. *Coord. Chem. Rev.*, **255**, 2514 (2011).
[15] Y.W. Shi, M.M. Shi, J.C. Huang, H.Z. Chen, M. Wang, X.D. Liu, Y.G. Ma, H. Xu, B. Yang. *Chem. Commun.*, **18**, 1941 (2006).
[16] P.E. Burrows, L.S. Sapochak, D.M. McCarty, S.R. Forrest, M.E. Thompson. *Appl. Phys. Lett.*, **64**, 2718 (1994).
[17] Y. Wang, W. Zhang, Y. Li, L. Ye, G. Yang. *Chem. Mater.*, **11**, 530 (1999).
[18] M. Goldman, E.L. Wehry. *Anal. Chem.*, **42**, 1178 (1970).
[19] T. Förster, K. Rokos. *Chem. Phys. Lett.*, **1**, 279 (1967).
[20] J.W. Eastman, E.J. Rosa. *Photochem. Photobiol.*, **7**, 189 (1968).
[21] Bruker SAINT-PLUS (including XPREP). Version 7.12, Bruker AXS Inc., Madison, WI (2004).
[22] L. Krause, R. Herbst-Irmer, G.M. Sheldrick, D. Stalke. *J. Appl. Cryst.*, **48**, 3 (2015).
[23] G.M. Sheldrick. *Acta Cryst.*, **A71**, 3 (2015).
[24] P. Müller. *Crystallogr. Rev.*, **15**, 57 (2009).
[25] K. Brandenburg, H. Putz, *DIAMOND. Release 3.0e.* Crystal Impact GbR, Postfach 1251, D-53002, Bonn, Germany (2004).
[26] M.M. Duvenhage, O.M. Ntwaeaborwa, H.C. Swart. *Phys. B: Condensed Matter*, **407**, 1521 (2012).
[27] J.A. Viljoen, H.G. Visser, A. Roodt. *Acta Cryst.*, **E67**, m1428 (2011).
[28] J.A. Viljoen, H.G. Visser, A. Roodt. *Acta Cryst.*, **E68**, m1344 (2012).
[29] S.S. Lo, W.H. Hsu, S.H. Sie, H.J. Leu. *J. Mater. Chem.*, **22**, 12618 (2012).
[30] R.J. Davey. In *Current Topics in Materials Science*, E. Kaldis (Ed.), Elsevier, Amsterdam, **8**, 429–479 (1982).
[31] Z. Berkovitch-Yellin. *J. Am. Chem. Soc.*, **107**, 8239 (1985).
[32] V.V.N. Ravi Kishore, A. Aziz, K.L. Narasimhan, N. Periasamy, P.S. Meenakshi, S. Wategaonkar. *Synth. Met.*, **126**, 199 (2002).
[33] W. Stampor, J. Kalinowski, G. Marconi, P. Di Marco, V. Fattori, G. Giro. *Chem. Phys. Lett.*, **283**, 373 (1998).
[34] M.M. Duvenhage, H.C. Swart, O.M. Ntwaeaborwa, H.G. Visser. *Opt. Mater.*, **35**, 2366 (2013).